

PAPER • OPEN ACCESS

Numerical investigations of small diameter two-phase closed thermosyphon

To cite this article: Y Naresh and C Balaji 2016 *J. Phys.: Conf. Ser.* **745** 032122

View the [article online](#) for updates and enhancements.



IOP | ebooks™

Bringing together innovative digital publishing with leading authors from the global scientific community.

Start exploring the collection—download the first chapter of every title for free.

Numerical investigations of small diameter two-phase closed thermosyphon

Naresh Y¹, Balaji C².

Heat Transfer and Thermal Power laboratory, Indian Institute of Technology Madras, Chennai, India.

²E-mail: balaji@iitm.ac.in

Abstract. In this work, a CFD model is developed to simulate the working of a 6mm diameter two-phase closed thermosyphon using water as the working fluid. At each section (evaporator, condenser, adiabatic) of the thermosyphon, lumped equations have been developed to calculate the temperatures at corresponding sections. In order to process two phase flow inside the system, a user-defined function (UDF) has been developed and integrated with the CFD model. The volume of fluid (VOF) method is used to carry out the simulations in Ansys FLUENT 15 and the lumped equations are solved in MATLAB 2013a. Volume fractions and temperature profiles obtained from CFD simulations and the lumped parametric estimations are found to be in good agreement with the experimental results available in literature.

Introduction

Thermal management plays a critical and essential role in maintaining high efficiency and reliability of electronic components. Heat pipe technology that utilizes the phase change latent heat of working fluid and transfers the high heat flux from hot side to cold side is a very promising thermal management solution. A thermosyphon is a gravity assisted wickless heat pipe. A thermosyphon is a complex system which involves pool boiling, film condensation, convection, solid conduction and vapour flow, and is a formidable mathematical problem to solve.

Once the heat is supplied to evaporator wall, the liquid pool gets heated. Due to latent heat of evaporation of the working fluid phase change takes place at the evaporator, and the vapour thus generated at the evaporator moves in the upward direction due to density difference where it rejects the heat. The vapour gets condensed and falls back along the length of the condenser wall. A certain volume of evaporator is filled with the working fluid and the effect of filling ratio has been studied by Shabgard et al.[1]. The ratio of initial liquid pool volume to the evaporator volume is known as the filling ratio in a thermosyphon system. Jouhara and Robinson [2] carried out an experimental study on small diameter two-phase closed thermosyphon charged with water, FC-84, FC-77 and FC-3283. Out of all the working fluids water was seen to give better thermal performance. Fadhl et al. [3,4] carried out similar studies for simulating the two phase closed thermosyphon system by using water, R134a and R404a. For a wicked heat pipe Ferrandi et al. [5] developed a lumped parameter model to study the transient behaviour of the heat pipe. For small diameter tubes, Chowdhury et al. [6] developed correlations for boiling heat transfer. To predict the heat transfer coefficients within the evaporator pool empirical correlations are generally used. The heat transfer coefficient between the wall and the pool has been given among others, by Shiraishi et al. [7]. The heat transfer coefficient in the evaporator region and in the condenser region have been predicted by researchers in the past [see, for example 8,9].

For low filling ratio the evaporator part dries out easily while for higher fill ratio the active condenser area is not sufficient for heat removal. Based on these conditions an optimum filling ratio has to be used for better thermal performance of the heat pipe. In the present work, (i) a lumped model has been developed together with CFD simulation for capturing finer details of the flow and heat transfer.

² Email: balaji@iitm.ac.in



Water has been used as the working fluid and the results are validated with experimental results available in literature. Because of the limitation on the Courant number at the interfaces in VOF model, the time step used in the computations is 0.0001 s. For the system to reach steady state, the VOF model takes an inordinately long CPU time. Hence, there is a need for developing a tool to which reduces the computational time. With a lumped parametric model this can be achieved.

Model

A copper tube with a length of 200mm, having 12mm outer diameter and thickness is 3mm used as a closed thermosyphon system. The diameter which is considered in the present study is 6mm, can be considered as quite small compared with the thermosyphons reported in the literature. A thermosyphon consists of evaporator section of length 40mm, 100mm of the adiabatic section and 60mm of condenser section. The geometry is the same as the one used Jouhara and Robinson [2] and hence their experimental results are used to validate the present numerical work. The geometrical details of the model and key thermophysical properties used are given in Table 1.

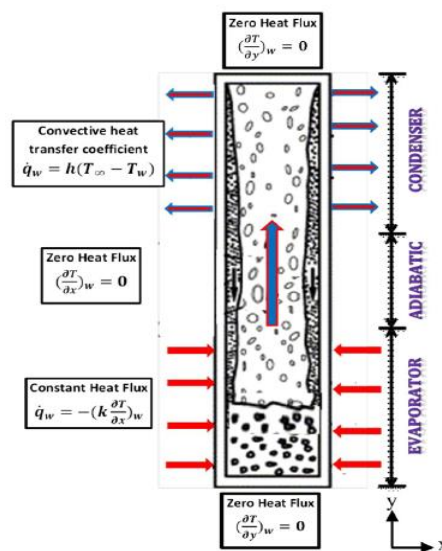


Figure 1. Two phase closed thermosyphon[3]

Volume of fluid (VOF) model

The VOF formulation relies on the fact that two or more fluids (or phases) are not interpenetrating. The sum of the volume fractions of all the phases in each control volume is equal to unity. The interface between the phases are not stationary, and in view of this the physical properties changes at the interfaces, thereby leading to an enormous amount of computational time to calculating them.

$$\alpha_L = 1; \text{ if each cell is filled with water.}$$

$$\alpha_L = 0; \text{ if each cell is filled with vapour.}$$

The sum of liquid volume fraction α_L and vapour volume fraction α_V equals unity at the interfaces [10]. Fadhl et al. [3, 4] expressed the density and surface tension of water as functions of temperature. The following equations are used for the calculation of surface tension along the liquid vapour interface and the density of the liquid respectively [11].

$$\sigma_{LV} = 0.09805856 - 1.845 \times 10^{-5} T - 2.3 \times 10^{-7} T^2 \quad (1)$$

$$\rho_L = 859.0083 + 1.252209T - 0.0026429T^2 \quad (2)$$

Table 1. Input parameters for numerical modelling as in Jouhara and Robinson [2]

parameter	value	Unit
Evaporator length	40	mm
Adiabatic length	100	mm
Condenser length	60	mm
Inner diameter	6	mm
Wall thickness	3	mm
Thermal conductivity of copper	350	W/mK
Specific heat of copper	385	J/KgK
Thermal conductivity of water	0.67	W/mK
Viscosity of water	2.2×10^{-4}	Pa s

Governing Equations

The following governing equations are used for the full numerical (CFD) model

Conservation of mass

$$\frac{\partial \rho}{\partial t} + \nabla \cdot \rho \vec{u} = S_M \quad (3)$$

Conservation of Momentum

$$\frac{\partial}{\partial t} (\rho \vec{u}) + \nabla \cdot (\rho \vec{u} \vec{u}) = \rho \vec{g} - \nabla p + \nabla \cdot \left[\mu (\nabla \vec{u} + \nabla \vec{u}^T) - \frac{2}{3} \mu \nabla \cdot \vec{u} \right] + S_{Fi} \quad (4)$$

Where S_{Fi} is continuum surface force: $S_{Fi} = 2\sigma_{lv} \frac{\alpha_l \rho_l c_v \nabla \alpha_v + \alpha_v \rho_v c_l \nabla \alpha_l}{\rho_l + \rho_v}$

σ_{lv} is surface tension coefficient, α is volume fraction.

Conservation of energy

$$\frac{\partial}{\partial t} (\rho e) + \nabla \cdot (\rho e \vec{u}) = \nabla \cdot (k \cdot \nabla T) + \nabla \cdot (\rho \vec{u}) + S_E \quad (5)$$

In the above equations, S_M is the mass source used to calculate mass transfer during the evaporation and the condensation, S_E is the energy source term used to calculate heat transfer during the evaporation and condensation and I is the unit vector. The source terms which are used in the UDF (user defined function) [3] for the simulation are given by

Mass transfer in evaporation:

$$S_M = -0.1 \rho_L \alpha_L \frac{T_{mix} - T_{sat}}{T_{sat}} \quad \text{For liquid phase} \quad (6)$$

$$S_M = 0.1 \rho_L \alpha_L \frac{T_{mix} - T_{sat}}{T_{sat}} \quad \text{For vapour phase} \quad (7)$$

Mass transfer in condensation:

$$S_M = 0.1 \rho_v \alpha_v \frac{T_{sat} - T_{mix}}{T_{sat}} \quad \text{For liquid phase} \quad (8)$$

$$S_M = -0.1 \rho_v \alpha_v \frac{T_{sat} - T_{mix}}{T_{sat}} \quad \text{For vapour phase} \quad (9)$$

Heat transfer in evaporation:

$$S_E = -0.1 \rho_L \alpha_L \frac{T_{mix} - T_{sat}}{T_{sat}} LH \quad (10)$$

Heat transfer in condensation:

$$S_E = 0.1\rho_v\alpha_v\frac{T_{sat}-T_{mix}}{T_{sat}}LH \quad (11)$$

Where LH is the latent heat 2455 kJ/kg, T_{sat} is the saturation temperature, T_{mix} is mixture temperature. In the UDF, the latent heat and saturation temperature of water are defined, the saturation temperature of water varies with inside saturation pressure. The boundary conditions are heat flux at the evaporator and the heat transfer coefficient at the condenser. These are obtained from experimental results reported in literature [2]. S_M the mass source and S_E the energy source as defined in the UDFs, are added to the mass and energy equations in FLUENT 15 respectively.

The lumped parameter model

A lumped parameter model [Figure 1] is used to compare its performance with experimental results. The resistance network model for the fluid involves lumps that are connected to each other by resistances and capacitive elements. The assumptions are one dimensional flow, the properties of vapour can be calculated by ideal gas equation, the phase change phenomenon (evaporation and condensation) are confined to their particular zones. For lumped modelling three zones are taken evaporator, condenser and adiabatic zone. All are connected by resistances.

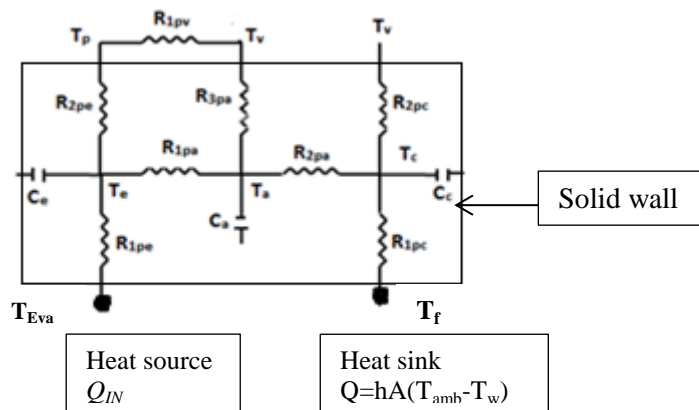


Figure 2. Network scheme for (solid model) present study

Table 2: Input parameters to lumped model for the present study following Jouhara and Robinson [2]

Symbol	Type
R_{1pe}, R_{2pe}	Radial resistances offered by evaporator wall
R_{1pa}, R_{2pa}	Axial resistances offered by solid wall
R_{1pc}, R_{2pc}	Radial resistances offered by condenser wall
R_{1pv}	Axial resistance offered by evaporator pool
R_{3pa}	Radial resistance offered by adiabatic wall
R_p, R_f	Radial resistances offered by pool at evaporator and fluid at condenser
C_e	Evaporator thermal capacitance
C_a	Adiabatic thermal capacitance
C_c	Condenser thermal capacitance.

The heat balance equations for the wall and the fluid are

$$C_e \frac{dT_e}{dt} = Q_{IN} - \frac{T_e - T_a}{R_{1pa}} - \frac{T_e - T_p}{R_{2pe} + R_p} \quad (12)$$

Where Q_{IN} is the heat input, T_e is evaporator wall temperature, T_a adiabatic wall temperature, T_p pool temperature, the node T_p is representing for entire pool temperature, R_p is radial resistance between evaporator wall and pool, $R_p = 1/hA$, where h is boiling heat transfer coefficient [7].

$$C_c \frac{dT_c}{dt} = \frac{T_a - T_c}{R_{2pa}} + \frac{T_v - T_c}{R_{2pc}} - \frac{T_c - T_f}{R_{1pc} + R_f} \quad (13)$$

Where R_f is convection resistance at condenser, T_f is external fluid temperature at condenser, T_c is condenser wall temperature. R_{1pc} is Radial resistance offered by condenser wall = $\frac{\ln \frac{r_o}{r_i}}{2\pi k l_c}$

$$C_a \frac{dT_a}{dt} = \frac{T_e - T_a}{R_{1pa}} - \frac{T_a - T_c}{R_{2pa}} - \frac{T_a - T_v}{R_{3pa}} \quad (14)$$

$$C_p \frac{dT_p}{dt} = \frac{T_e - T_p}{R_{2pe} + R_p} - \frac{T_p - T_v}{R_{1pv}} \quad (15)$$

$$T_v = \frac{\gamma - 1}{\gamma} \frac{T_v}{P_v} \frac{dP_v}{dt} \quad (16)$$

$$C_v \frac{dP_v}{dt} = M_e - (M_c + M_a) \quad (17)$$

Where P_v is vapour pressure

The rate of evaporation of from the evaporator pool is given by

$$\frac{dM_e}{dt} = \frac{T_p - T_v}{R_{1pv}} \quad (18)$$

The rate of change in the pool mass is

$$\frac{dM_p}{dt} = (M_c + M_a) - M_e \quad (19)$$

The rate of accumulation of vapour is

$$\frac{dM_v}{dt} = M_e - (M_c + M_a) \quad (20)$$

Where M_c is condensed fluid mass in kg/s, M_e is evaporated fluid mass in kg/s, M_a is mass in adiabatic section in kg/s.

The rate of mass transfer in the adiabatic section is

$$\frac{dM_a}{dt} = \pm \frac{T_v - T_a}{R_{3pa}} \quad (21)$$

Positive sign is used if $T_a < T_{sat}$ and negative sign is used if $T_a > T_{sat}$. The resistances and capacitances used in the above equations are defined in Table 2.

Numerical procedure

To solve the above system of equations numerically, all the unknowns are placed in the form of a column vector

$$y = \{T_e, T_a, T_p, T_c, T_v, T_f, M_e, M_a, M_c, M_p\}^T \quad (22)$$

The set of conditions for the ordinary differential equation is

$$\begin{aligned} \frac{dy}{dt} &= f(t, y) \\ y(t_0) &= y_0 \end{aligned} \quad (23)$$

By using finite difference Euler's method, the equations are discretised explicitly as

$$y^{n+1} = y^n + hf(t^n, y^n) \quad (24)$$

For the full numerical simulations of the thermosyphon system (i.e. CFD simulations) the VOF model has been used. An optimum mesh size of 40,256 (computational mesh number in fluent) quad, map cells was selected for present study. The Euler-Euler approach has been adopted here because it uses the phasic volume fraction. Transient simulations have been carried out with a time step of 0.0001s. The SIMPLE algorithm for pressure velocity coupling and second order upwind scheme for momentum and energy, Geo-Reconstruct and PRESTIO for volume fraction and pressure are used in the simulations. In this study, the residuals are set to a value of 10^{-5} for convergence for all the equations.

Numerical Results:

For a power level of 120.5W the volume fractions of the pool boiling in the evaporator and film condensation over the surface of the condenser are shown in Figs 3 and 4. The blue colour indicates the fluid, while the red colour indicates the presence of vapour. In fluent water vapour is taken as primary phase (phase 1) and water liquid is taken as secondary phase (phase 2). The contours which are shown in figure 3 are phase 1 volume fractions. In the legend view if the value is one (red colour), it means complete vapour and if the value is equal to zero (blue colour), it means complete liquid. At the beginning, 60% volume of evaporator is filled with water. Constant heat flux boundary condition is applied at the evaporator section. Once the fluid temperature reaches the defined saturation temperature in the UDF, the liquid starts to change phase. After 5 s the vapour slowly enters into the adiabatic region, and as time progress the vapour reaches the condenser. A thin layer of liquid film has been observed during the process of condensation as shown in Fig 4.

Temperature contours during the operation of thermosyphon system are shown in Fig 5 for a input of 120.5W. Because of the evaporation, the temperature contours are seen to "grow" due to the movement of vapour in upward direction which can be seen at 10s. After 20s, there is not much variation in temperature inside the as seen in Fig 5. The performance of the thermosyphon is characterized by its thermal resistance. The overall heat transfer rate is given by

$$Q = \frac{T_{eva_{avg}} - T_{con_{avg}}}{R_{th}} \quad (25)$$

The CFD simulation results reach steady state around 60s and lumped simulations reach to steady state around 120s. The temperature distribution along the outer wall of thermosyphon for two heating power levels of 120.5W and 220W are shown in figs 6 and 7 respectively. The distance between 0 and 40mm indicates the evaporator section, the distance between 40mm and 140mm indicates the adiabatic section, the distance between 140mm and 200mm indicates the condenser section. Six different positions have been used to monitor the temperatures for the evaporator, condenser and adiabatic sections. For a power level of 180W, both CFD and lumped analysis are done. The CFD simulation results and lumped parametric estimations showed the same trend as the experimental data. From fig 6 the average relative error of evaporator, adiabatic and condenser average temperatures in the full numerical (CFD simulations) are 2.09%, 3.17% and 2.41% respectively, in lumped are 1.19%, 1.44% and 2.4% respectively. The lumped parameter model and CFD results are in good agreement with the experimental results. Because of the small time step CFD model takes enormous amount of computational time, this calls for the need to develop a more simple and quick computational tool to simulate the characteristics of a thermosyphon system. This is achieved by lumped modelling, though this is a little compromise on the accuracy.

Fig 8 shows the variation of thermal resistance for three different power levels of 120.5, 180, and 220W. As the value of power level increases the total thermal resistance of the thermosyphon will decrease, as expected which indicating better thermal performance. Results which are shown in figures 6, 7 and 8 are steady state results.

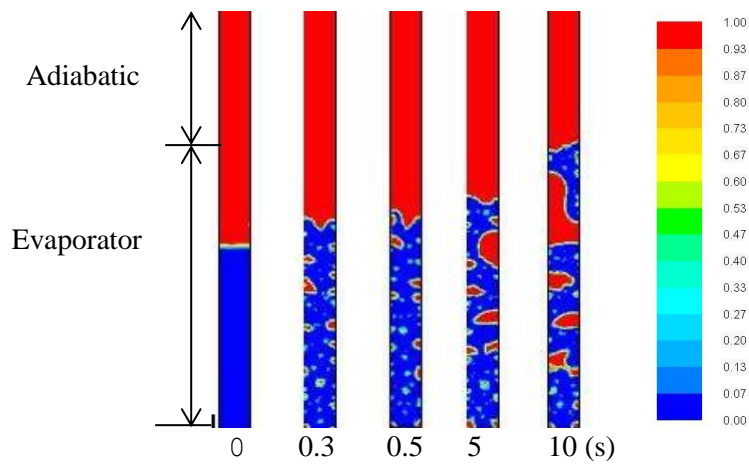


Figure 3. Pool boiling in evaporator at different times for 120.5W power level (Phase-1 volume fractions)

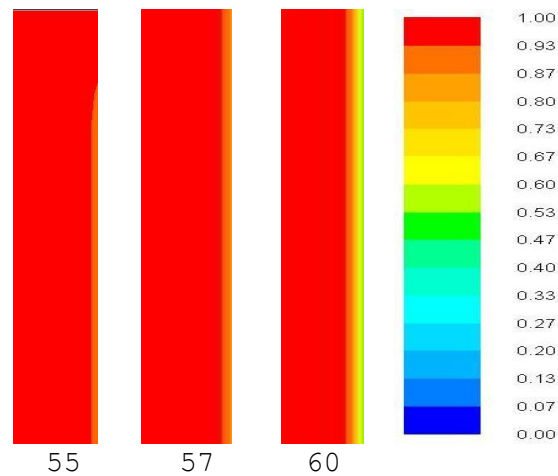


Figure 4. Liquid film condensation at the condenser section for 120.5W power level (Time in s)

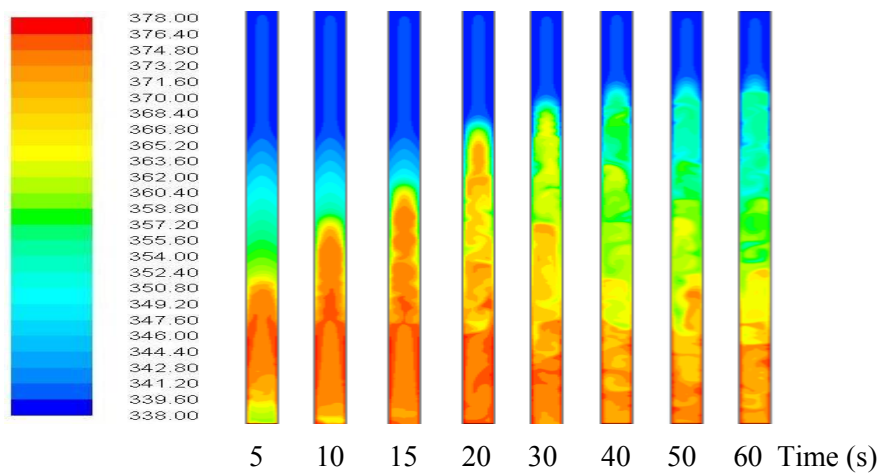


Figure 5. Temperature contours at different time steps for 120.5W power level

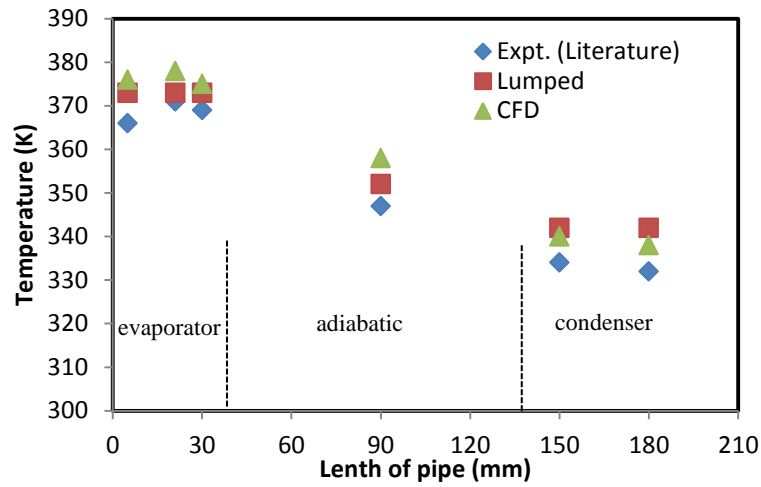


Figure 6. Variation of temperature along the length of heat pipe for a power level of 120.5W.

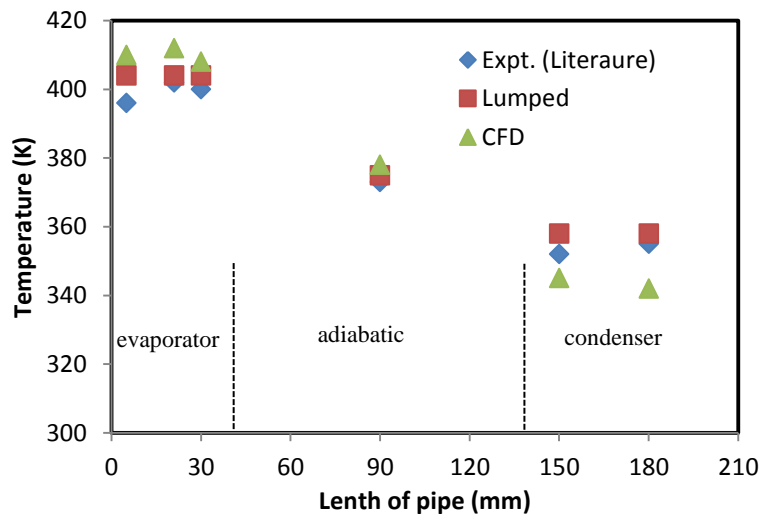


Figure 7. Variation of temperature along the length of heat pipe for a power level of 220W.

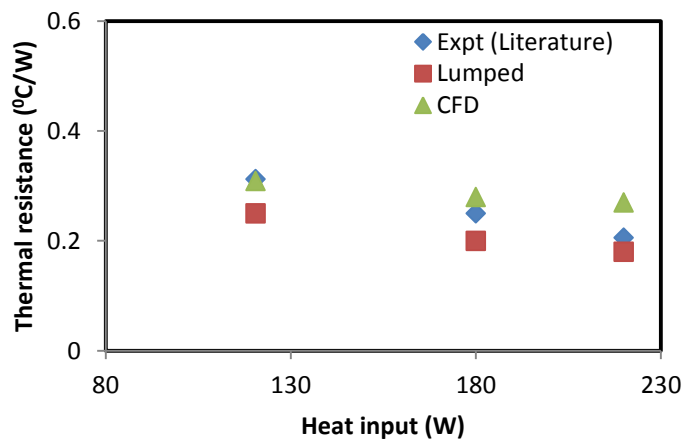


Figure 8. Variation of thermal resistance for different heat inputs

Conclusions:

This paper presented the results of a numerical investigation of small diameter two phase closed thermosyphon system by using both full numerical simulations (CFD) and lumped modelling. The full numerical solutions (CFD) consist of phase change simulations at evaporator and condenser. UDFs that calculate mass and energy source terms were input to ANSYS Fluent in order to simulate phase change phenomenon. With the VOF model and UDF functions, the phase change process has been successfully simulated. Because of small time step size due to limitation of Courant number, the computational times are enormous. Hence, lumped equations were developed at various sections of the thermosyphon system and these equations are discretised by using finite difference method. The system of equations was solved to study the transient behaviour of the heat pipe.

Numerical results obtained from both the approaches are compared with experimental results available in literature and it was seen that good agreement exists between numerical and experimental results. For calculation of gross quantities like thermal resistance and axial variation of temperature across the thermosyphon, the lumped model would suffice. However, to get finer details like liquid fractions contours and flow velocities, the full CFD model is required. The two can be intelligently used in tandem to critically evaluate the thermal performance of the thermosyphon with a view to optimizing it.

References:

1. Shabgard, Hamidreza, Bin Xiao, Amir Faghri, Ramesh Gupta, and Walter Weissman. Thermal characteristics of a closed thermosyphon under various filling conditions. *International Journal of Heat and Mass Transfer* 70 (2014): 91-102.
2. Jouhara, Hussam, and Anthony J. Robinson. Experimental investigation of small diameter two-phase closed thermosyphon charged with water, FC-84, FC-77 and FC-3283. *Applied thermal engineering* 30, no. 2 (2010): 201-211.
3. Fadhl, Bandar, Luiz C. Wrobel, and Hussam Jouhara Numerical modeling of the temperature distribution in a two-phase closed thermosyphon. *Applied Thermal Engineering* 60, no. 1 (2013): 122-131.
4. Fadhl, Bandar, Luiz C. Wrobel, and Hussam Jouhara. "CFD modelling of a two-phase closed thermosyphon charged with R134a and R404a." *Applied Thermal Engineering* 78 (2015): 482-490.
5. Ferrandi, C., F. Iorizzo, M. Mameli, S. Zinna, and M. Marengo. Lumped parameter model of sintered heat pipe: Transient numerical analysis and validation. *Applied Thermal Engineering* 50, no. 1 (2013): 1280-1290.
6. F.Md. Chowdhury, F. Kaminaga, K. Goto, K. Matsumura, Boiling heat transfer in a small diameter tube below atmospheric pressure on a natural circulation condition, *Journal of Japan Association for Heat Pipe* 16 (1997) 14–16.
7. Shiraishi, M., K. Kikuchi, and T. Yamanishi. Investigation of heat transfer characteristics of a two-phase closed thermosyphon. *Journal of Heat Recovery Systems* 1, no. 4 (1981): 287-297.
8. G.S.H. Lock. *Latent Heat Transfer: An introduction to fundamentals*, Oxford Science publications., Oxford University Press, US, 1996.
9. F.P. Incropera and D.P. Dewitt. *Fundamentals of heat transfer*, John Wiley, New York, 2009.
10. ANSYS FLUENT, Theory guide 13.0, Multiphase flows, Ansys Inc., November 2010, pp, 455-568 (chapter 17).
11. Yunus A. Cengel, Michael A. Boles, *Thermodynamics: an engineering approach*, McGraw-Hill, New York 2011.